

Applying statistical rock physics and seismic inversions to map lithofacies and pore fluid probabilities in a North Sea reservoir.

Tapan Mukerji^{*1}, Arild Jørstad², Gary Mavko¹, and John Reidar Grant¹

¹Rock Physics Laboratory, Dept. of Geophysics, Stanford University, CA 94305.

²Statoil R & D center, Trondheim, Norway.

Summary

Reliably predicting lithologic and saturation heterogeneities is one of the key problems in reservoir characterization. In this study we show how statistical rock physics techniques combined with seismic information can be used to classify reservoir lithologies and pore fluids. One of the innovations was to use a new seismic impedance attribute (related to V_P/V_S ratio) that incorporates far-offset data, but at the same time can be practically obtained using normal incidence inversion algorithms. The methods were applied to a North Sea turbidite system. We incorporated well log measurements with calibration from core data to estimate the near and far-offset reflectivity and impedance attributes. Multivariate probability distributions were estimated from the data to identify the attribute clusters and their separability for different facies and fluid saturations. A training data was set up using Monte Carlo simulations based on the well log derived probability distributions. Fluid substitution by Gassmann's equation was used to extend the training data, thus accounting for pore fluid conditions not encountered in the well. Seismic inversion of near offset and far offset stacks gave us two 3-D cubes of impedance attributes in the interwell region. The near offset stack approximates a zero offset section giving an estimate of the normal incidence acoustic impedance (ρV). The far offset stack gives an estimate of a V_P/V_S related elastic impedance attribute that is equivalent to the acoustic impedance for non-normal incidence. These impedance attributes obtained from seismic inversion were then used with the training probability distribution functions to predict the probability of occurrence of the different lithofacies in the interwell region. Simple statistical classification techniques, as well as geostatistical indicator simulations were applied on the 3-D seismic data cube. A Markov-Bayes technique was used to update the probabilities obtained from the seismic data by taking into account the spatial correlation as estimated from the facies indicator variograms. The final results are spatial 3-D maps of not only the most likely facies and pore fluids, but also their occurrence probabilities. A key ingredient in this study was the exploitation of physically-based seismic-to-reservoir properties transforms optimally combined with statistical techniques.

Introduction

Modern seismic imaging techniques provide a powerful means of visualizing the internal geometry of the heterogeneous subsurface. Sources of reservoir heterogeneity include variations in lithology, porosity, and pore fluid properties. They control not only the amount of hydrocarbons that may be present, but also their recoverability from distributed reservoir compartments. Indeed, these reservoir heterogeneities are one of the primary causes of low hydrocarbon recovery efficiency resulting in poor sweep, early breakthrough, and pockets of by-passed oil.

Numerous interpretation techniques have emerged to map this rock and fluid spatial variability. These techniques include estimates of lithology, porosity, and saturation made from geologic, log, and seismic data. Many of these mappings employ powerful multivariate statistical techniques. Other more deterministic techniques are based on the extensive laboratory and theoretical work on distinct physical relations between rock/fluid parameters and measurable acoustic properties. There is also evidence that, when properly scaled, these relations apply to well-log data as well. However, in the interwell region, the fewer constraints provided by seismic data alone lead to greater uncertainty in the 3D seismic-to-rock properties transforms. This work presents a strategy for estimating the uncertainty and mapping the probability of occurrence of different facies and fluids in the interwell region by combining attributes from seismic impedance inversion with statistical rock physics.

The geological setting is a Tertiary turbidite system in the North Sea. The system was covered by a 3-D seismic survey which was specially processed for amplitude interpretation. The well information is sparse within the coverage of the 3-D survey. Emphasis was on careful analysis of the well data for calibration, and use of the exhaustive seismic data for lithofacies characterization.

Defining lithofacies from logs

We first defined seismic lithofacies representing seismic scale sedimentary units with distinguishable characteristic petrophysical properties such as clay content, bedding configuration (massive or

Mapping lithofacies probabilities

interbedded), grain size, cementation, density, and seismic velocities. This was the basis for quantitative facies and fluid estimation from seismic data. A key well was identified with a complete suite of good quality logs that sampled all or most of the important lithologies in the turbidite system. Well logs play the important role of linking rock parameters to the exhaustive seismic data. Figure 1 shows an example of some of the important logs from the key well.

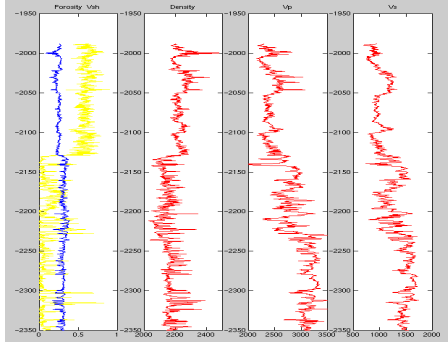


Fig. 1. Porosity, volume shale (light curve), density, V_p and V_s logs from one of the wells used in this study.

Based on the logs, and some core and thin section descriptions, 5 major facies were identified. Facies II-V [II-thick bedded sands; III-interbedded sand-shale; IV-silty shales; V-pure shales] represent a gradual transition from clean sandstones to pure shale. Gravels and conglomerates were included as facies I. Brine sands and oil sands were grouped as separate categories. The gamma ray log values and patterns, and velocity and density logs were used primarily to determine the different facies with contrasting seismic properties.

Pore fluid effects

An important complicating factor is the presence of flushed zones in hydrocarbon columns at the wells. Because of the water based drilling fluid, the well logs could be potentially measuring water saturated values from the mud-filtrate invaded zone, instead of measuring the oil zone. This was carefully investigated using deep and shallow resistivity and Gassmann modeling of dry ultrasonic data with actual mud-filtrate and reservoir hydrocarbon properties. The fluid substitution showed that log values in the oil facies were actually very close to the water saturated values. Comparison of log and core porosities, and empirical V_p/V_s relations also confirmed that the sonic velocities were measures of the water saturated facies and not oil saturated rocks. Using the log data alone to build up our calibration probability distribution functions (pdfs) would not capture the properties of the oil saturated facies. A key step therefore was to extend the log derived training data, using Gassman's equations, to incorporate

velocity and impedance attributes not encountered in the well. This augmented training data was then used to build up the calibration pdfs. Figure 2 shows reflectivity at 0° and 30° , $R(0)$ versus $R(30)$, for brine sands and oil sands with a shale cap rock. The non-normal reflectivity $R(30)$ was calculated using Aki-Richards approximation. Velocities and densities for the sands were drawn from the well log derived pdfs.

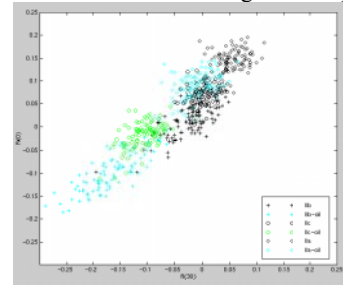


Fig. 2. Reflectivities at 0° (y-axis) vs. 30° (x-axis): brine sands (black markers), oil sands (light markers).

Acoustic and Elastic Impedance

Ambiguities in lithologic and fluid identification based only on normal incidence impedance (ρV) can often be effectively removed by adding information about V_p/V_s related attributes. This provides the incentive for AVO analysis. Synthetic seismic modeling has shown that sometimes it can be difficult to use the seismic amplitudes quantitatively due to practicalities of picking and resolution problems. Another approach to lithofacies identification is based on seismic impedance inversion. Usually this is applied to zero offset or near offset sections to estimate the acoustic impedance ρV , and therefore does not contain V_p/V_s information. Here we define a pseudo impedance attribute which is a faroffset equivalent of the more conventional zero offset impedance. We will call this the elastic impedance as it contains information about the V_p/V_s ratio. This approach allows us to use the same algorithm for inversion of far offset stack as the near offset stack, and get an elastic impedance cube. The inversion for this pseudo impedance parameter is therefore economical and simple, with no additional software required.

The acoustic impedance, ρV , can be expressed as:

$$I_a = e^{2\int R(0)dt} \quad (1)$$

where $R(0)$ is the 0° normal incidence reflectivity. Similarly, the elastic impedance is defined in terms of the reflectivity at θ° , $R(\theta)$ as (Granli, 1997):

$$I_e(\theta) = e^{2\int R(\theta)dt} \quad (2)$$

Using one of the well known approximations for $R(\theta)$ (e.g. Aki & Richards, 1980) in terms of V_p , V_s and

Mapping lithofacies probabilities

density contrasts, I_e can be expressed in terms of layer parameters available from logs as:

$$I_e(\theta) = V_P^{1+\tan^2\theta} \rho^{1-4\left(\frac{V_S}{V_P}\right)^2 \sin^2\theta} - 8\left(\frac{V_S}{V_P}\right)^2 \sin^2\theta V_S \quad (3)$$

Figure 3 shows the seismic lithofacies defined from the wells and by fluid substitution, in an I_e - I_a cross plot. Facies that overlap in acoustic impedance can be discriminated by their elastic impedance and vice versa.

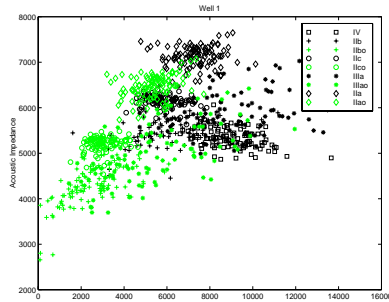


Fig. 3. Cross plot of elastic impedance at 30° versus acoustic impedance for different lithofacies. Light markers indicate oil saturated facies.

Seismic inversions

The seismic data used in this study are near offset and far offset stacks (Figure 4 shows an example) from a marine 3D survey covering approximately 300 km² of the North Sea. The near offset traces have an average incidence angle of 8° at the target level, while the far offset stack has an average incidence angle of 26° .

The post stack inversion was performed using a commercially available package. The inversion requires as inputs information about the seismic wavelet, the geometric structure from structural seismic interpretation, and a prior model based on well log impedance. The same method (generalized least squares inversion) is used for both the near and far offset stacks, except that the calculated elastic impedance logs for the proper incidence angle were used as the prior model for the far offset inversions. We used two independent methods to obtain a reliable wavelet estimate. The first method, provided in the software package, is based on the amplitude spectrum of a selected time window, and a scan of the phases to pick one that best matches synthetic and true seismic traces. Another independent estimate, outside the package, was obtained from the Akaike information criterion (AIC) estimate (e.g. Priestley, 1983) of the filter that best minimises the error between synthetic and real traces. Both methods indicated that the actual wavelet at the target level was mixed phase with a time shift of ~ 20 ms. The prior model was created by extrapolation of well data along the

defined structural horizons. The inversion itself is a 1-D trace-by-trace inversion, based on convolution with the wavelet. Figure 5 shows impedance cubes from the inversions.

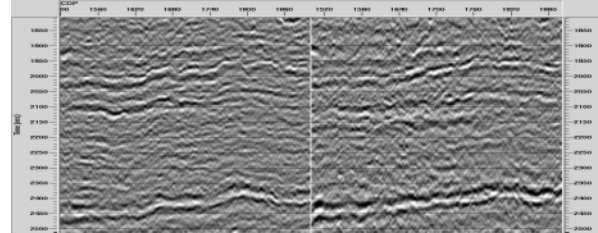


Fig. 4. Near (left) and far (right) offset stacked sections.

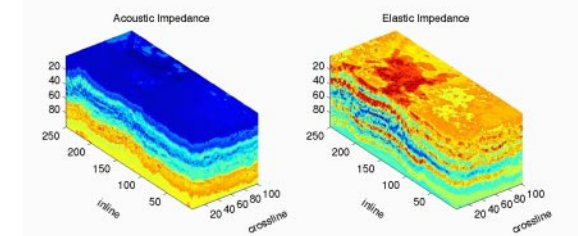


Fig. 5. Acoustic (left) and elastic (right) impedance cubes.

Statistical classification and simulation

The impedance attribute cubes were used to estimate the most likely facies, and the probability of occurrence of each facies at every grid point within the cube. We used three different statistical approaches: a linear discriminant analysis (e.g. Fukunaga, 1990) based on the Mahalanobis distance, a probability estimate based on the complete pdfs for each facies calibrated from the training data, and a geostatistical indicator simulation approach, incorporating the spatial correlation of the facies as described by their variograms. In general, all three methods gave similar probability maps for the different facies. As a first step, we compared the log values and the inverted acoustic and elastic impedances traces co-located with the wells as a check for consistency. The co-located impedance traces were then used to classify the known facies at the wells. This was done with the standard Mahalanobis distance method, which takes into consideration only the means and covariances of the training pdfs. Figure 6 shows the classification success at the wells for two cases: classifying facies using the inverted I_a alone, versus using I_e in addition to I_a . The histograms clearly show, by the increased classification success, the value of using elastic impedance.

In addition to the linear discriminant classification, we also used the complete pdfs to estimate $P(\text{facies} | I_a, I_e)$, the conditional probability of occurrence of each facies at each point in the 3-D cube, given the inverted

Mapping lithofacies probabilities

acoustic and elastic impedances. Figure 7 shows a simplified contour plot of the calibration pdfs used as inputs, and Figure 8 displays slices of the estimated conditional probability maps for different facies.

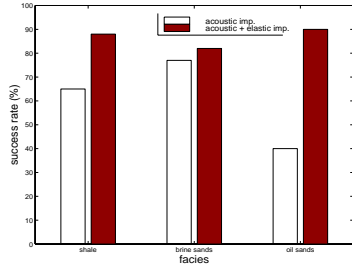


Fig. 6. Classification success rate at the wells.

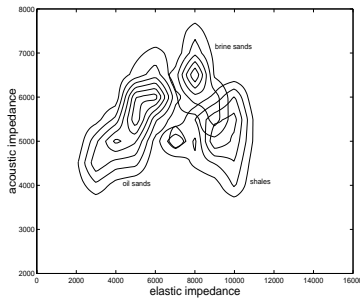


Fig. 7. Contour plot of I_a - I_e bivariate pdfs.

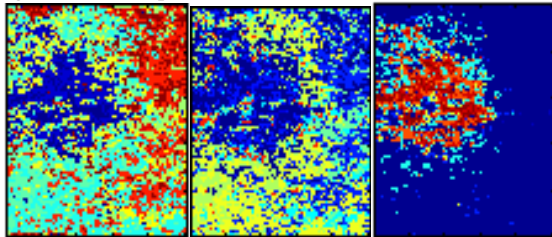


Fig. 8. Horizontal time slices showing the conditional probabilities of occurrence of shales (left), brine sands (center), and oil sands (right) within the seismic grid.

Geostatistical indicator simulation provided multiple equiprobable realizations of facies and fluid distributions in the reservoir. The Markov-Bayes indicator formalism (Deutsch & Journel, 1996) was used to obtain the posterior conditional pdfs, incorporating the spatial correlations of the facies as estimated from the facies indicator variograms. This updates the prior pdf, $P(\text{facies} | I_a, I_e)$ to give the posterior pdf, $P(\text{facies} | I_a, I_e, \text{well indicator data})$, shown along vertical sections in Figure 9. The well coverage was very sparse, and the variogram model for facies indicators along the horizontal direction had to be completed by borrowing the spatial anisotropy ratio from variograms of the seismic impedance. Hence the updating did not change the prior pdfs significantly.

Conclusion

This paper shows how near and far offset seismic impedance attributes can be optimally combined with well log calibration, and statistical rock physics to classify and map the occurrence probabilities of reservoir lithofacies and fluids. The methods are applied to a North Sea reservoir to obtain the most likely interpretation as well as assess the uncertainty of the interpretation.

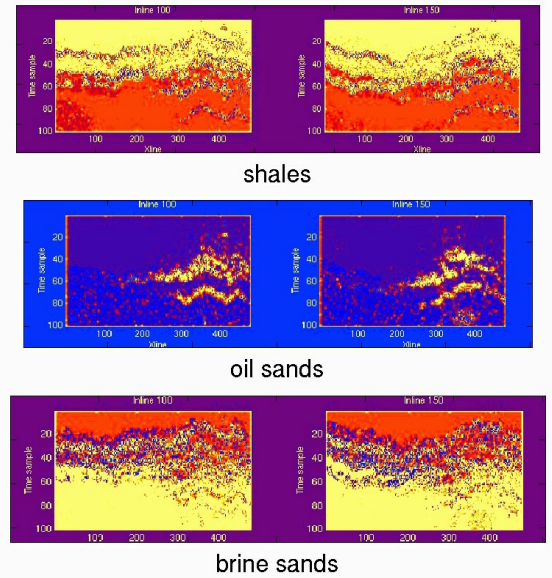


Fig. 9. Vertical sections along two in-lines showing probability of shales (top), oil sands (center), and brine sands (bottom). Light color indicates higher probability.

Acknowledgements

This work was supported by Stanford Rock Physics project and Statoil who provided all the data.

References

- Aki, K., and Richards, P. G., 1980, Quantitative Seismology, Freeman W. H. & Co.
- Deutsch, C. V., and Journel, A. G., 1996, GSLIB: Geostatistical software library and user's guide, 2ed., Oxford University Press.
- Fukunaga, K., 1990, Introduction to statistical pattern recognition, 2ed., Academic Press.
- Granli, J. R., 1997, Lithology and fluid phase prediction from seismic data, Statoil report.
- Priestley, M. B., 1983, Spectral analysis and time series, Academic Press.